THE ASTROPHYSICAL JOURNAL, 475:L33–L36, 1997 January 20


# COHERENT RADIATION PATTERNS SUGGESTED BY SINGLE-PULSE OBSERVATIONS OF A MILLISECOND PULSAR

J. G. ABLES[1] AND D. MCCONNELL
Australia Telescope National Facility, CSIRO, Locked Bag 194, Narrabri, NSW 2390, Australia
A. A. DESHPANDE
Raman Research Institute, Bangalore, India
AND
M. VIVEKANAND
National Centre for Radio Astronomy, Pune, India
*Received 1996 July 18; accepted 1996 October 31*

## ABSTRACT

We have observed intense radiation spikes from the millisecond pulsar PSR J0437−4715 and find their distribution in pulsar spin phase to be quite unlike the integrated pulse profile. The spikes are observed almost exclusively in a 10° phase window centered on the main pulse. Within that window the phase distribution has a periodic variation, producing a pattern reminiscent of the diffraction fringes associated with coherent emission from a finite aperture. We propose a source model in which the spikes are emitted coherently from a region with spatial scale ≈100 m.

*Subject headings:* pulsars: individual (PSR J0437−4715) — radiation mechanisms: nonthermal

## 1. INTRODUCTION

It is known that the radio emission from pulsars is produced by a coherent mechanism, since, if the emission is treated as a purely random process, the inferred temperature is $\gg 10^{23}$ K, which seems impossible. The early discovery that the radio emission is often polarized and that the change of polarization angle during the pulse is simply related to the projection of the line of sight on the direction of a rotating magnetic dipole field (the so-called single-vector model; Radhakrishnan & Cooke 1969) further supports a coherent mechanism. Classical coherence implies that individual charged particles move in a collective manner so that bulk currents are established. The radiation field and the currents are, of course, linked by Maxwell's equations. With sufficient knowledge of the field, the distribution of the currents in time and space can be deduced. Even when full details of the field are not known, examination of any *diffractive* patterns in the emission would, at the very least, yield the spatial scale of the currents and highly constrain the feasible geometries. Unfortunately, no observations ascribed to diffraction have ever been reported. This lack has given free scope to the large number of divergent theories of the radio emission of pulsars in the current literature. (For an extensive review see Beskin, Gurevich, & Istomin 1993.)

We report here a new phenomenon, associated with the extraordinary radiation spikes seen in a bright millisecond pulsar, that is difficult to explain as anything but the effect of diffraction. The associated spatial scale is ≈100 m. This scale plus the simple and persistent appearance of the pattern are incompatible with the widespread view (e.g., Melrose 1993) that the pulsar radio emission is the result of the incoherent addition of many small (∼1 m) coherent emitters. We give a simple model of a current distribution in time and space with a computed field that closely fits the detail of the observed radiation pattern of the spike emission. This model is based on a radially expanding charge disk with a bulk outward motion from the star of Lorentz factor $\gamma = [1 - (v/c)^2]^{-1/2} \sim 6$. The model also predicts a polarization sweep of the spike radiation exactly like that of the single-vector model.

## 2. OBSERVATIONS AND DATA REDUCTION

We observed the millisecond binary pulsar PSR J0437−4715 (Johnston et al. 1993) (spin period 5.758 ms, orbital period 5.74 days, dispersion measure DM = 2.65 pc cm$^{-3}$, distance ∼100 pc) almost every day in the interval 1995 March 2–March 20, using the recently upgraded Ooty radio telescope (Selvanayagam et al. 1993). The signal (one linear polarization, bandwidth ≈10 MHz, center frequency $\nu_0 = 326.5$ MHz) was analyzed by a digital spectrometer (1024 channels of ∼10 kHz width), which also provided on-line, postdetection de-dispersion (McConnell et al. 1996). The observed mean peak flux was ∼1 Jy, but for a small percentage of the time reached ∼10 Jy for ∼10 m intervals owing to strong-focusing scintillation (intrinsic variations may also contribute). During these brightenings, unbroken sample streams (sample interval $t_s = 102.4$ μs) of ∼70 s were recorded, separated by unrecorded intervals of ∼30 s. Altogether, 44 such data sets in four groups on four separate days were obtained.

The most striking feature of the pulses observed (Fig. 1, *top*) is that many have a very strong (≫ mean peak flux), narrow (unresolved at $t_s = 102.4$ μs) "spike" of emission near the maximum of one or more of the three principal peaks of the mean pulse profile. Here we discuss only the spikes associated with the central, highest peak, these being by far the most numerous. Expected interstellar scattering time (Lang 1980) is ≲1 μs, and so the true widths could be ≪100 μs. Nyquist reconstruction (Bracewell 1965) allows exact recovery of the underlying band-limited continuous function (pulsar signal plus noise) from our samples (Fig. 1, *bottom*), and from this

[1] On secondment from the Division of Radiophysics, CSIRO, Australia.

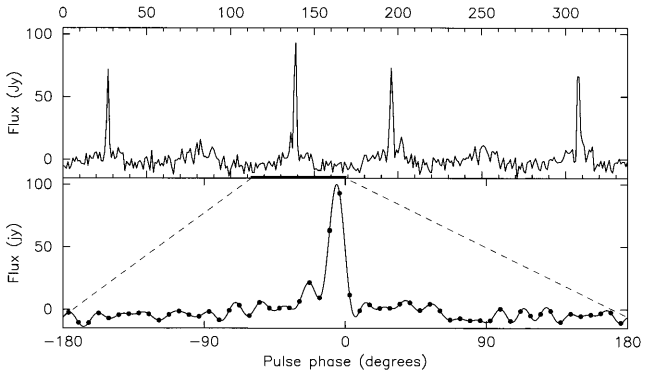


FIG. 1.—*Top*: Typical segment of raw sample data. Individual samples have been connected with straight lines. One pulsar period is 56.2 samples. Six periods are shown, four of which show narrow spikes of radiation. These spikes are about a third of the height of the largest seen in the whole data set. *Bottom*: Nyquist reconstruction of the third (from the left) pulse, the full period of which is marked with the heavy bar in the top panel. Filled circles mark the original samples. The reconstructed spike is essentially equal in width to the instrumental impulse response time, so that the true width must be less. The *time* of the peak, however, can be recovered to a fraction of the sample interval.

function the relative times of arrival (TOAs) of the spikes were found. Monte Carlo analysis indicates that these times are accurate to $\sim 5$ $\mu$s ($\sim t_s/20$). Using a computed ephemeris with recent timing parameters (Bell et al. 1995), the TOAs were reduced to pulsar rotational phases so that each spike could be represented as a single point in a phase-amplitude scatter diagram. For each 70 s record, the distribution of the 500 largest spikes was convolved (smoothed) with a unit-amplitude Gaussian of 4 $\mu$s FWHM (smaller timescales are meaningless because of our $\sim 5$ $\mu$s jitter). The number 500 was chosen as a compromise between using only large pulses with small TOA jitter and having enough pulses to make a well-defined distribution.

All distributions show a smooth peak with FWHM $\approx 150$ $\mu$s (10° longitude) modulated by fringes with about nine fairly evenly spaced subpeaks (Fig. 2). To see whether the subpeaks are the result of the "drifting subpulse" phenomenon (Ruderman & Sutherland 1975) seen in some long-period pulsars, we examined longitudinally resolved power spectra for secondary periodicities (Backer 1973) and spike phase-time scatter diagrams for the characteristic diagonal banding (Backer 1973) that drifting subpulses produce. No evidence of subpulse drifting was found.

## 3. A COHERENT RADIATION MODEL

Here we have the very surprising result that the mean profile of the spike component shows a periodic fringe structure. This is strongly reminiscent of the diffraction pattern of a sharply bounded finite aperture, which leads us to propose the following emission model. Consider (Fig. 3) a thin ($\ll \lambda_0 = c/\nu_0$) charge sheet of diameter $D$ moving outward at a velocity $v \lesssim c$ near the surface of the neutron star and along the magnetic polar axis of the oblique-rotator pulsar model (Radhakrishnan & Cooke 1969; Komesaroff 1970), as was first suggested by Sturrock (1971). The charges are constrained to follow the field lines, and the energy in the field is so high that it is unperturbed by any reaction forces from the charged particles. The field lines diverge. The charge disk is radially stretched, causing a radial current $\boldsymbol{j}(t)$. The electromagnetic field radiated is proportional to $\partial \boldsymbol{j}/\partial t$, which, at every point in the disk,

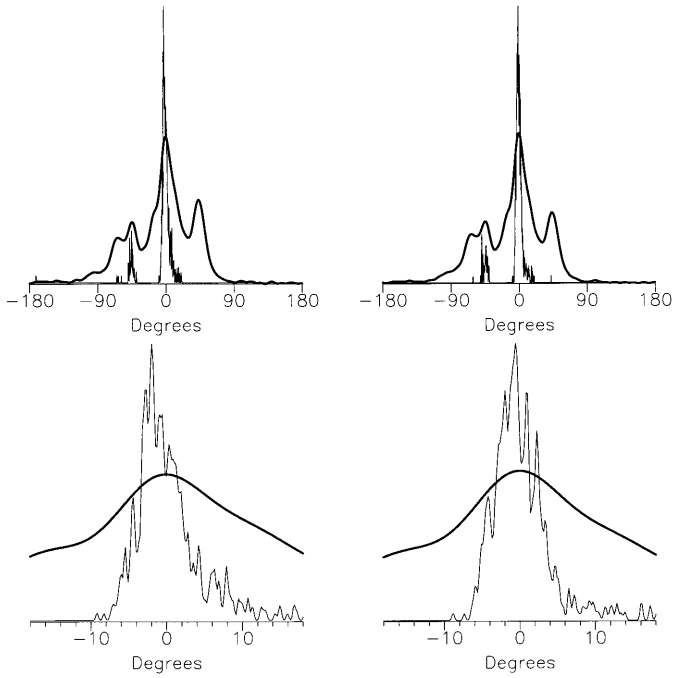


FIG. 2.—Results of analysis of two data sets (*left and right columns*). *Top*: Mean pulse profile (*heavy line*) for the entire data set and a smoothed TOA distribution using only the 500 largest spikes (the narrow profiles). Both profiles are normalized, the mean total flux profile by dividing by the number of periods used ($\sim$12,000) and the spike component profile by dividing by the number of spikes (500). In this Letter we examine only the spikes associated with the central component of the mean profile. *Bottom*: Expansion of the central part of the spike component profile above. Fringing of the spike component profiles is evident, but with some change in detail between the sets, which were separated by 30 minutes. The mean fringe spacing $\delta\theta$ (as determined by power spectrum analysis of the profiles) was $1\overset{\circ}{.}20 \pm 0\overset{\circ}{.}03$ (*left*) and $1\overset{\circ}{.}29 \pm 0\overset{\circ}{.}03$ (*right*). The FWHM overall widths $\Delta\theta$ of the distributions are estimated as $5\overset{\circ}{.}6 \pm 0\overset{\circ}{.}1$ (*left*) and $6\overset{\circ}{.}1 \pm 0\overset{\circ}{.}1$ (*right*). Note that in these distributions there is almost no "noise" in the traditional sense, the spikes being much larger than the radiometer noise and many of them combining to form a typical fringe subpulse. At low levels the variance is dominated by "counting noise" resulting from the low density of spikes.

is proportional to the product of the charge density and field curvature.

We computed the emission pattern of such a disk as seen in the observer's frame and compared it with the spike TOA distribution. The calculation proceeds in three steps. First, the far-field radiation pattern is found in the frame comoving with the charge sheet, the wavelength used being related to the observer's wavelength by the relativistic Doppler formula. Second, the pattern is found in the observer's frame by using the relativistic aberration formula. Finally, the effect of gravitational bending of electromagnetic waves near the surface of the neutron star is taken into account to arrive at the observed "antenna pattern" of the radiating charge sheet.

Using spherical-polar coordinates ($\theta$, $\phi$), with $\theta$ the polar angle from the direction of $\boldsymbol{v}$ and $\phi$ the azimuthal angle in the plane normal to $\boldsymbol{v}$, the far electric field is

$$\boldsymbol{E}(\theta) \propto \int_0^{D/2} \frac{\partial \boldsymbol{j}(r)}{\partial t} J_1(kr \sin\theta) r\, dr,$$

where $\boldsymbol{j}(r)$ is the radial current in the plane of the charge disk, $r$ is the radial distance from the center of the disk, $J_1$ is the first-order Bessel function, and $k = 2\pi/\lambda$. Due to the azi-

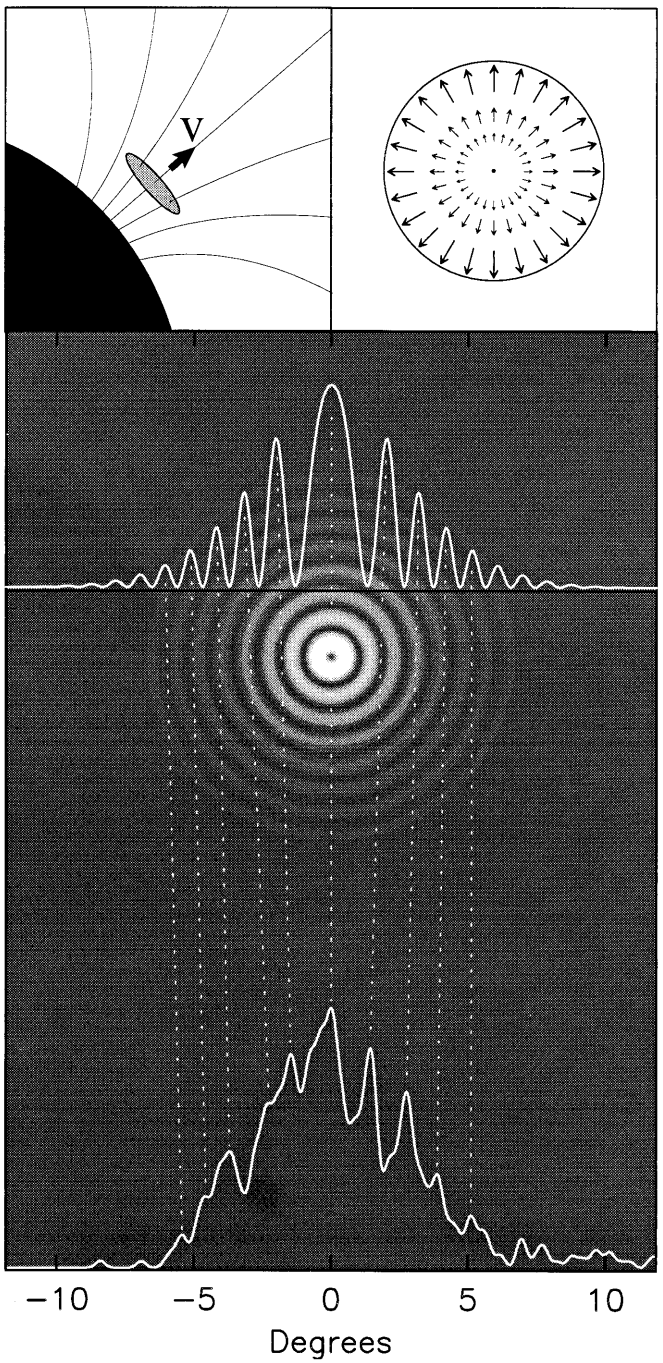


FIG. 3.—Summary of the model. A circular sheet of charge is accelerated in the magnetic polar region (*top left*) and moves away from the star at $v \approx c$. Charges within the sheet are constrained to follow the field lines, and so the sheet stretches; the resulting radial current vectors are shown schematically (*top right*). Below is shown the diffraction pattern for the best-fitting parameters given in the text with the resulting profile along the observer's line of sight, which agrees with previously published polarization data (Manchester & Johnston 1995). Note that the chosen line of sight does *not* pass through the center of the diffraction pattern. At the point of closest approach it becomes tangential to a bright diffraction ring, causing the central fringe to be broadened. Shown at bottom for comparison is the observed spike component profile of Fig. 2 (*right*). Broadening of the central fringe is evident. Fringe visibility is reduced by the spike timing noise of $\sim 5$ $\mu$s (the spacing between fringes corresponds to $\sim 22$ $\mu$s) and may also be reduced by variations in the source location and diameter during the 70 s integration.

muthal symmetry of the current distribution, $\boldsymbol{E}(\phi) = 0$. The observer's wavelength $\lambda_0$ is related to the comoving wavelength $\lambda$ by the relativistic Doppler formula, so that $\lambda = \lambda_0(1 - \beta^2)^{1/2}/(1 + \beta \cos \theta_0)$. Here $\beta = v/c$, and $\theta_0$ is the polar angle at which the observer sees radiation with polar angle $\theta$ in the comoving frame. The angles are related by $\cos \theta = (\cos \theta_0 + \beta)/(1 + \beta \cos \theta_0)$ and $\sin \theta = \sin \theta_0(1 - \beta^2)^{1/2}/(1 + \beta \cos \theta_0)$.

Correction is now made for the bending of rays away from the normal due to the gravitational field of the neutron star. For a neutron star of mass $1.4\ M_\odot$ and emission at $R = 10$ km (the nominal stellar radius) there is an almost uniform stretching of the pattern by a factor $\approx 1.3$ for $\theta \leqslant 0.1$, decreasing to $\approx 1.18$ for $R = 15$ km.

Finally, the angular distribution of radiated power in the observer's frame is given by $P(\theta_0) \propto (d\theta/d\theta_0)^2 |E(\theta_0)|^2$, the factor $(d\theta/d\theta_0)^2$ being required for conservation of flux assuming a flat spectrum.

We speculate that the rapidly moving charge sheet could be related to the following picture of the pulsar emission region (after the polar cap model of Sturrock 1971, and as worked out in more detail by Ruderman & Sutherland 1975). The polar cap is the surface region around a magnetic pole where the field lines do not close inside the velocity-of-light cylinder defined by the radial distance at which corotation with the pulsar gives a tangential velocity of $c$. Particles streaming on these field lines are not trapped in the pulsar's magnetosphere and can flow to infinity. Depletion of charges causes an insulating gap to form above the cap, and a significant portion of the homopolar generator potential ($\sim 10^{17}$ V) resulting from the spinning magnetic field appears across it. When the field strength grows to the point where spontaneous $e^{\pm}$ pair creation is energetically possible, the gap breaks down in a fast ($<1$ $\mu$s) cascade of electrons, positrons, and $\gamma$-rays. The plasma is constrained to expand outward along the field lines, driving at its leading edge the charge sheet we have proposed. After a recovery time (which may vary widely), this sequence recurs, each time producing one of the radio emission spikes we observe. From our observations of about one spike per pulsar period and their appearance in a $\sim 100$ $\mu$s time window, we infer that the true mean rate of spike emission is $\sim 10$ kHz.

In this model, each spike should emit a full diffraction (beam) pattern corresponding to the disk currents, but since the expected spike duration ($<1$ $\mu$s) is so much smaller than the time required for the diffraction pattern to be rotated through our line of sight, the full pattern is revealed only in our plots of the amplitude and rotational phase of many spikes.

The observed "fringe pattern" serves not only to delineate the overall size of the charge disk but also to indicate something of the radial charge distribution. To restrict the overall width of the computed fringe pattern to fit the observed pattern, we found it necessary to limit the charge distribution, and hence the current, to an annulus of width only $\sim 10\%$ of the disk radius.

The radial symmetry of the current disk centered on the magnetic pole results in a radiation null on-axis and a polarization angle that points to the pattern center from all positions within the pattern. Thus the polarization angle sweep will be exactly as described in curvature radiation (single-vector) models (Radhakrishnan & Cooke 1969; Komesaroff 1970). The pattern is composed of concentric rings with spacing in the observer's frame $\delta\theta \approx 1.3\lambda_0/D$. This spacing does not depend on the bulk-motion Lorentz factor $\gamma$. The overall width of the pattern $\Delta\theta$ is strongly determined by the

radial width of the current annulus and, to a lesser extent, by $\Delta\theta \lesssim 1/\gamma$. Allowing for the angles from the magnetic pole to the spin axis and to the observer's line of sight suggested by polarization data (Manchester & Johnston 1995), we find a good match to the observed pattern with $D = 110$ m, an annular charge width of 7 m, and $\gamma = 6$ (Fig. 3). By adjusting the width of the charge annulus, adequate matches to the observed pattern can be found with $2 < \gamma < 20$, but always an *annular* charge distribution was required for a reasonable fit. Such annuli also appear in the theory of the polar active region (Beskin et al. 1993).

The emission frequency spectrum $S(\nu)$ of a radiation spike is given by the squared magnitude of the Fourier transform of the current-pulse time profile. A current pulse with sudden onset and no subsequent decay (a step function in time) radiates a spike with $S \propto \nu^{-2}$. A finite rise time $t_r$ produces a steeper spectrum for $\nu \gtrsim 1/t_r$, while a fall time $t_f$ gives a low-frequency turnover at $\nu \sim 1/t_f$. Given this model, measurements of the frequency spectrum of radiation spikes will yield the current's temporal behaviour to go with the spatial description we have deduced.

## 4. CONCLUSION

It should be borne in mind that the present model is *only* for the impulsive, spike component of the radiation of J0437−4715 and that this component seems quite separate from the much wider and, in the mean, more intense radiation, the origin of which has not been addressed in this Letter. However, it has not escaped the authors' attention that this simple model, involving repetitive impulsive radiation from a large ($\gg\lambda_0$), coherent patch precisely located on the stellar surface, will have important ramifications for many hitherto puzzling aspects of the pulsar emission phenomenon, and that it also raises some controversial questions. Thus, it is most important to know whether these effects are found in other pulsars.

More observations are needed with better time resolution, especially submicrosecond resolution, which is possible only through coherent de-dispersion. This would allow the polarization of individual spikes to be measured, thus testing the prediction of the model. (Note that the existing polarization data [Manchester & Johnston 1995] is dominated in the mean profiles by the wide-angle emission.) Observations at other frequencies are important. However, the simple view that diffraction pattern widths should scale directly with wavelength may need modification if, for example, different wavelengths are emitted at different heights above the stellar surface.

We thank R. H. Frater for financial support for the construction of the digital spectrometer, R. J.-M. Grognard for consultation on relativity, and R. D. Ekers and M. J. Kesteven for critical reading of the manuscript. J. G. A. thanks D. N. Cooper for supporting his work at the ATNF. J. G. A. and D. M. are grateful for the hospitality of the Raman Research Institute (India) and the National Centre for Radio Astronomy (India) during the observations. Travel to India (J. G. A., D. M.) was funded by the Access to Major Research Facilities Program (Australia).

## REFERENCES

Backer, D. C. 1973, ApJ, 182, 245
Bell, J. F., Bailes, M., Manchester, R. N., Weisberg, J. M., & Lyne, A. G. 1995, ApJ, 440, L81
Beskin, V. S., Gurevich, A. V., & Istomin, Y. N. 1993, Physics of the Pulsar Magnetosphere (Cambridge: Cambridge Univ. Press)
Bracewell, R. 1965, The Fourier Transform and Its Applications (New York: McGraw-Hill)
Johnston, S., et al. 1993, Nature, 361, 613
Komesaroff, M. M. 1970, Nature, 225, 612
Lang, K. R. 1980. Astrophysical Formulae (Berlin: Springer)
Manchester, R. N., & Johnston, S. 1995, ApJ, 441, L65
McConnell, D., Ables, J. G., Bailes, M., & Erickson, W. C. 1996, MNRAS, 280, 331
Melrose, D. B. 1993, in Pulsars as Physics Laboratories, ed. R. D. Blandford, A. Hewish, A. G. Lyne, & L. Mestel (New York: Oxford Univ. Press), 105
Radhakrishnan, V., & Cooke, D. J. 1969, Astrophys. Lett., 3, 225
Ruderman, M. A., & Sutherland, P. G. 1975, ApJ, 196, 51
Selvanayagam, A. J., Praveenkumar, A., Nandagopal, D., & Velusamy, T. 1993, Inst. Electron. Telecommun. Eng. Tech. Rev., 10, 4
Sturrock, P. A. 1971, ApJ, 164, 529